# EXPERIMENTAL VALIDATION OF A SIMPLIFIED WELDING SIMULATION APPROACH FOR FATIGUE ASSESSMENTS

N. FRIEDRICH* and S. EHLERS*

*Hamburg University of Technology (Institute for Ship Structural Design and Analysis, 21073, Hamburg, Germany, nils.friedrich@tuhh.de)

DOI 10.3217/978-3-85125-615-4-46

ABSTRACT

The paper presents the application of a simplified approach for numerical welding simulations and its validation by means of residual stress measurements. The aim of the presented work is to provide a practical calculation method for welding residual stresses to assess their influence on the fatigue strength of welded structures. Welding simulations are relatively complex while their reliability is often uncertain. On the other hand, residual stress measurements frequently show wide scatter. The paper motivates the use of a simplified approach without calibration by experimental data, as it is applicable for fore- and hindcasting of residual stresses during the design phase or for failure analysis. The simulations are divided into a transient thermal analysis followed by a mechanical analysis. A simple prescribed temperature heat source with uniform temperatures is used to apply the welding energy. The results are validated with residual stress measurements by X-ray diffraction and hole drilling on three welded geometries: longitudinal stiffeners, K-butt welds and a structure-like component.

Keywords: simplified welding simulation; residual stress prediction; uniform temperature distribution; experimental validation; residual stress measurement; longitudinal stiffener; multilayer weld.

## INTRODUCTION

Direct consideration of welding residual stresses in engineering applications is still limited. Measurements are complex and not always possible. Welding simulations often do not prove very efficient considering modelling and computation effort opposed to accuracy and reliability of the results. On the one hand, non-linear simulations with a high temporary resolution will require long calculation times depending on the model size, load step number and computational capacities. On the other hand, modelling and setting up the simulation will require effort. This includes the calibration of the heat input in the thermal part of the analysis which is often considered a pre-requisite for reliable residual stress and distortion results [1]. It usually involves measuring temperatures during welding and taking macrographs from the weld cross-section. Simulation parameters are then iteratively adapted in order to match the calculated temperature distributions with the acquired experimental data. Although this procedure, applied e.g. in [1-5], seems straightforward,

when it comes to detail, differences may be observed in the practical execution. Sometimes peak temperatures are compared or the focus lays on the trend of the temperature curve after a few seconds of cooling. Distances from the weld at which temperatures are compared may vary significantly and for small distances it may be hard to accurately measure and transfer it to an idealized weld shape in the model. The molten weld bead in the macrograph or the heat affected zone may be matched with the respective isotherm from the simulation. The shape of the weld may be modelled in different detail. Different importance may be given to the element size close to the weld to be fine enough to capture the steep gradients in temperature (and in residual stresses as well). These none exclusive parameters will to some extend influence the outcome of the heat source calibration.

In [1] a bench mark study on uncertainties in welding simulations is presented and the importance of an accurate calibration is pointed out. But how relevant is a correct heat input really for the resulting residuals stresses? Does a careful and (apparently) accurate calibration guarantee reliable simulation results? Despite of being laborious, the need for experimental data limits the applicability of a simulation. Such calibration procedure is not practical during the design phase, when measurements are not yet be possible, or for the assessment of existing structures for which such data is not available. Simplified simulation approaches without calibration may be less accurate, but perhaps accurate enough for applications such as fatigue assessments affected by other parameters, which are often rough estimates only.

According to Goldak and Akhlaghi [6] the best heat source model to choose depends on how accurately the heat source should be modelled, on the objective of the modelling and on what information is available. To predict distortions and residual stresses in low alloy steel structures accurate temperatures below 600 to 800°C are described to be most important. Simplified simulation approaches for multilayer welds were studied in [5]. It was found that geometrical simplification of the modelled weld shape can produce good results in terms of residual stresses while reducing simulation times. Whereas, approaches aiming to reduce the number of calculated load steps (e.g. application of thermal cycles or lumping of weld passes) may produce poor results compared to transient simulations.

In [7] the authors adopted a simplified welding simulation procedure for metal active gas welding renouncing on experimental calibration to assess residual stresses in small-scale specimens for fatigue investigations. Instead of using an equivalent heat source with a volumetric power density distribution (e.g. according to [8]), a prescribed temperature heat source [6] with a uniform temperature on the weld cross section has been applied in a transient thermal analysis. In [7] the simulation approach was applied to a multilayer K-butt weld and the influence of different simulation parameters has been investigated. The aim of the present paper is to transfer the approach to the weld geometry of a longitudinal stiffener and to validate it by residual stress measurements on three different geometries including small-scale specimens and a structure-like component.

The objective is to provide a simulation procedure to calculate residual stresses and consider them in the fatigue assessment of welded structures. It should be applicable also if no detailed data of the welding process is available. For fatigue assessments residual stresses transversal to the weld, at the weld toe are most important as possible cracks will initiate here.

# SIMULATION APPROACH

## GENERAL PROCEDURE

The applied finite element simulation approach consists of a transient thermal analysis followed by a nonlinear structural analysis. A uniform temperature distribution is applied to the weld cross-section and moved along the weld, instead of using a volumetric heat source with a power density distribution (Fig. 1). Prescribed temperature heat sources are described in [6] and have been applied e.g. in [9-10]. The procedure used in the present paper was described in [7] and will be summarized shortly in the following.

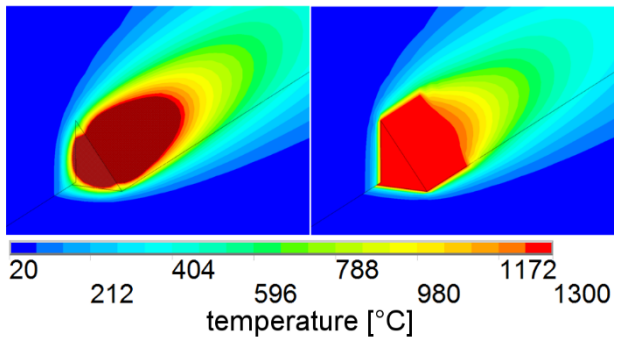


**Fig. 1** Volumetric heat source (left) and uniform temperature (right) applied on a fillet weld [7].

In the thermal analysis a temperature of 1300°C is applied to a short section of the simulated weld. At each time step, this section is moved by the assumed welding speed of 7.8 mm/s. The time step size is 0.5 seconds, respectively 0.25 seconds for portions of the weld closest to the investigated region e.g. for fatigue assessments. Elements of the simulated welds are deactivated at the beginning of the simulation and are activated as the temperature is applied to them. For each time step the temperature distribution in the model is calculated considering radiation and convection on its surfaces according to the analytical formulas given in [11].

In the structural analysis the same time steps as before are calculated. The temperature distributions from the thermal analysis are applied as loads to calculate residual stresses and distortions. Effects of phase transformation are considered by using two different curves for the thermal expansion coefficient for heating and cooling on the weld elements. The curve used for cooling showing an expansion between 400 and 500°C. The yield strength is reduced in the same temperature interval to account for transformation-induced plasticity (TRIP).

## PARAMETER VARIATION

The simulations are performed without calibration by experimental data. Therefore, a variation of the simulation parameters was performed to verify if and how they may affect simulation results. In [7] this was done for a multilayer cruciform joint. As a result, it was found that a variation of the applied temperature or the assumed welding speed (i.e. of the heat input) did not significantly affect the resulting transversal residual stresses in front of the weld.

In the following the simulation approach described above was applied to the model of a longitudinal stiffener. Simulation parameters were varied to assess the influence for this particular weld geometry.

### *FE-Model*

Modelling and simulation were done using the finite element (FE) software ANSYS Mechanical 15.0. The model of a small-scale specimen with a longitudinal stiffener used for the parameter variation is shown in Fig. 2. It consists of 8 node solid elements. Elements size was 0.25 mm in front of the weld toe at the end of the stiffener and coarser on the rest of the model. Temperature-dependent material data for S355 steel from [12] was used assuming kinematic hardening. The young's modulus was increased to 215 GPa to improve the stability of the simulations. Constrains were applied to three nodes only to avoid rigid body motion.

It was assumed that the welding starts and ends at half length of the stiffener.

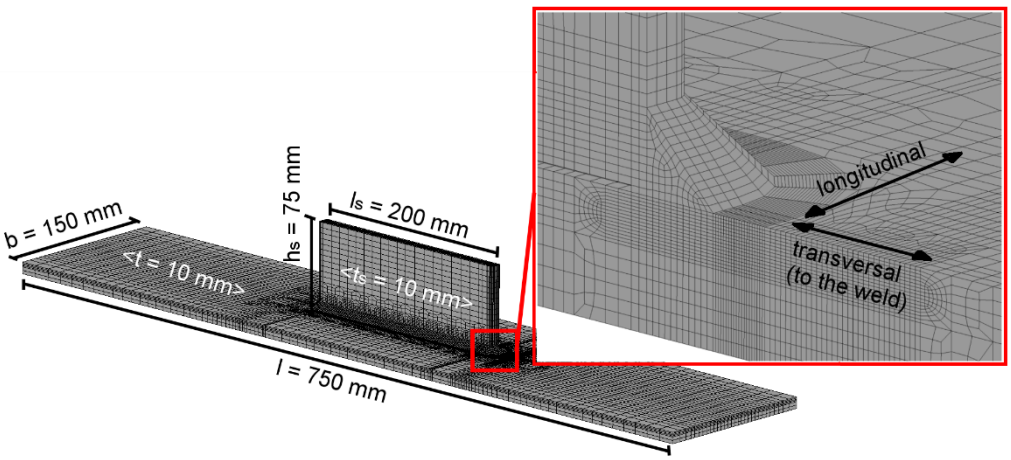


**Fig. 2** Dimensions of the fe-model and definition of directions with respect to the weld at the end of the stiffener.

### *Applied temperature*

The temperature applied to the weld cross-section was varied between 1000 and 1500°C. The resulting residual stresses in front of the weld toe at the end of the stiffener are shown

in Fig. 3. The directions transversal and longitudinal are referred to the weld at the end of the stiffener as defined in Fig. 2. For temperatures of 1400°C and more the cut-off temperature above which the elements are deactivated had to be below 1200°C in order to run the simulations. In the diagram this is indicated by a dashed line.

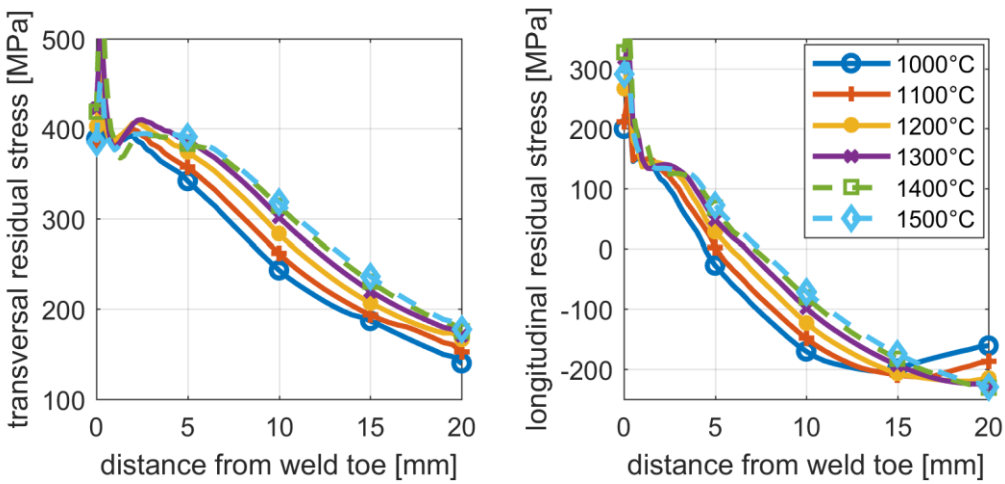


**Fig. 3** Calculated residual stress depending on the temperature applied to the weld elements (dashed line: cut-off temperature lower than applied temperature).

The curves for both directions (transversal and longitudinal) show a steep increment on the first element from the weld toe. At the weld toe, the elements of the weld are activated as they cool below the applied temperature while the adjacent elements are always active. At the moment of the activation, large deflections can occur in the neighbouring elements, which at that point present elevated temperatures themselves and thus low stiffness. This may cause a peak in the resulting residual stresses at the first node in front of the weld toe. Moreover, the weld toe is not modelled with a radius and thus shows a sharp notch. This represents a singularity in the FE-model, which will cause an unrealistic stress concentration at the weld toe. The residual stress values on the first elements, up to approximately 1 mm from the weld toe, should therefore not be evaluated and will not be considered in the following.

Neglecting the peak at the first node from the weld toe, transversal residual stresses reach a value of about 400 MPa some millimetres from the weld with decreasing tendency towards the weld toe. In longitudinal direction values of approximately 150 MPa are reached. With increasing temperatures, the curves become wider and the residual stresses decrease farther from the weld.

All in all, the residual stress curves and the highest values in front of the weld differ only little depending on the applied temperature. This is in agreement with the findings for the cruciform joint in [7]. For the following simulations a temperature of 1300°C was applied.

*Throat thickness*

The throat thickness of the weld was varied between 3.0 and 6.5 mm. With an increasing weld cross section more thermal energy is applied to the model and thus the heated volume undergoing shrinkage during cooling is larger. The resulting residual stresses in front of the weld toe at the end of the stiffener are shown in Fig. 4.

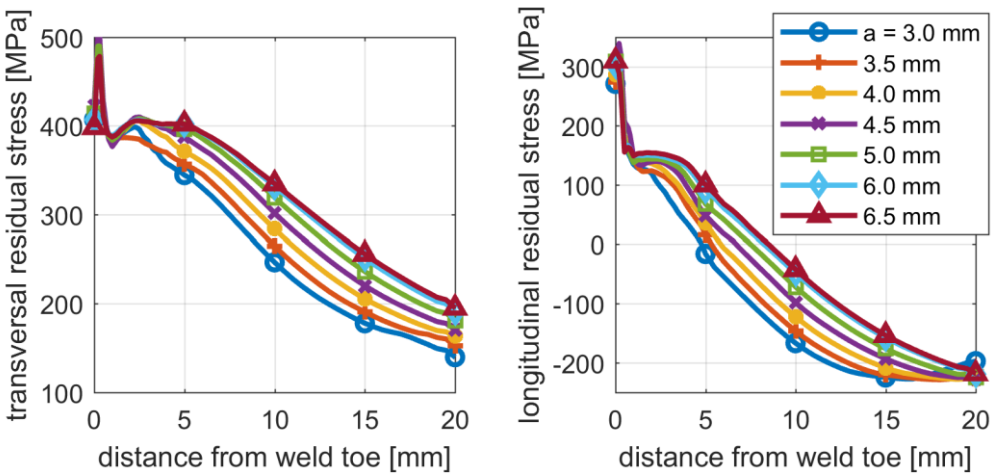


**Fig. 4** Calculated residual stress depending on the throat thickness $a$.

Analogue to the results with varied temperatures, the curves become wider and the residual stresses decrease farther from the weld as the throat thickness increases. The highest values reached in front of the weld differ only little depending on the throat thickness. For the following simulations a throat thickness of 4.5 mm was applied.

*Phase transformation temperature interval*

As described in section 2.1 phase transformation is considered by using two different curves for the thermal expansion coefficient for heating and cooling. On all weld elements the same curve is used for cooling, independently of the reached peak temperature and cooling time. The temperature interval in which the phase transformation and thus a volume expansion is assumed during cooling was varied between 300 and 700°C. The resulting residual stresses are shown in Fig. 5. The results include those from simulations without phase transformation (with straightened thermal expansion curve as for an austenitic steel) and with the same thermal expansion curve as for heating (austenite phase transformation between 700 and 900°C). The assumed temperature interval for phase transformation shows no influence on the calculated residual stresses in front of the weld. As described above, it was not possible to evaluate the simulation results at the weld toe.

For the following simulations phase transformation during cooling was assumed between 400 and 500°C. According to experimental results in [13] this should be a realistic range and has yielded satisfying results for a K-butt weld in [7].

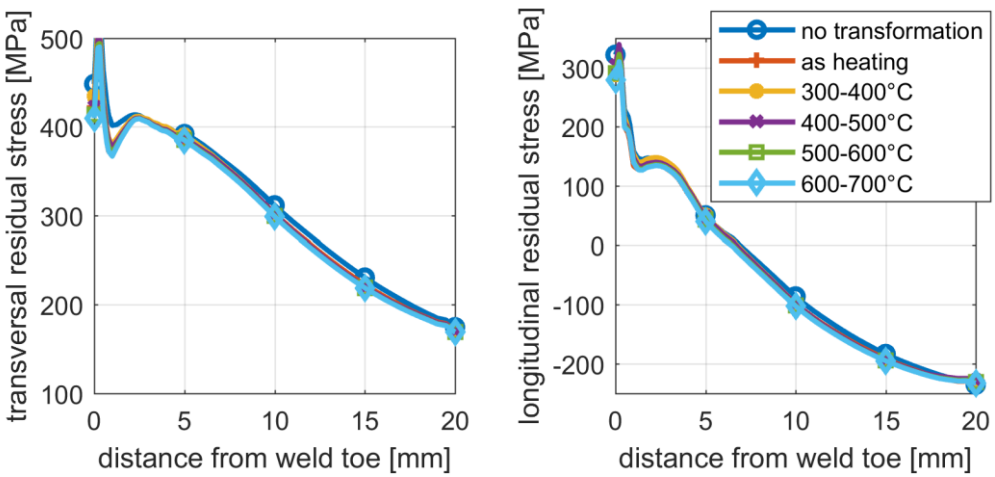


**Fig. 5** Calculated residual stress without phase transformation and depending on the temperature interval for phase transformation.

*Yield strength*

The yield strength was varied between 385 and 470 MPa. Temperature dependent material data, including stress-strain curves, for S355 was taken from [12]. At room temperature these showed a yield strength of approximately 385 MPa. Tensile tests (at room temperature) were performed on steel of grade A36 and S460 showing yield strengths of 430 and 470 MPa, respectively. Stress-strain curves for elevated temperatures of the S355 were adapted by scaling the yield strength with the ratio of yield strengths at room temperature. The elastic-plastic zone was scaled by the ratio of the difference between yield limit and tensile strength. All other material properties, including young's modulus, were kept the same for all simulations. The resulting residual stresses are shown in Fig. 6. In transversal direction the maximum reached residual stresses increases with the yield strength of the material.

For the following simulations material properties of the S355 were assumed.

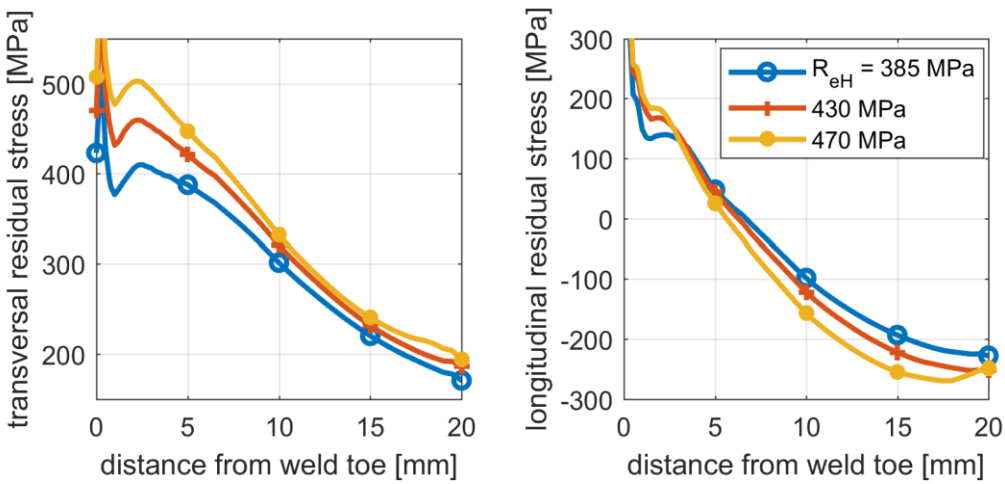


**Fig. 6** Calculated residual stress depending on the yield strength $r_{EH}$.

## EXPERIMENTAL VALIDATION

To validate the simulation results the calculated residual stresses were compared to measurements on three different welded geometries:

- Small-scale specimen with a longitudinal stiffener
- Small-scale specimen with a multilayer K-butt weld
- Large-scale component including a multilayer cruciform joint and a longitudinal stiffener.

### LONGITUDINAL STIFFENER

The geometry of the longitudinal stiffener specimens is shown in Fig. 7. The specimens were made of steel S355J2+N. The base plates were cut from a 10 mm plate using a band saw. Tensile tests gave the following values: yield strength $R_{p0.2}$ = 370 MPa; tensile strength $R_m$ = 543 MPa; Young's modulus $E$ = 201 GPa. Flat bars 40x10 (S355) were used for the stiffeners. Manual metal active gas (MAG) welding was applied. Welding started at the left end of the stiffener (referred to Fig. 7). Welding current was 250 A and voltage 29 V. During welding the ends of the specimens were fixed on a square tube 80x80x3.5 by screw clamps to reduce distortion. The clamps were removed after the specimens had cooled below 100°C (measured by infrared thermometer). To allow hole drilling measurements close to the weld toe, on a number of specimens the right end of the stiffener was cut at a 45° angle before welding (see Fig. 7). According to simulations, residual stresses in the base plate should have been the same as in specimens with straight stiffeners.

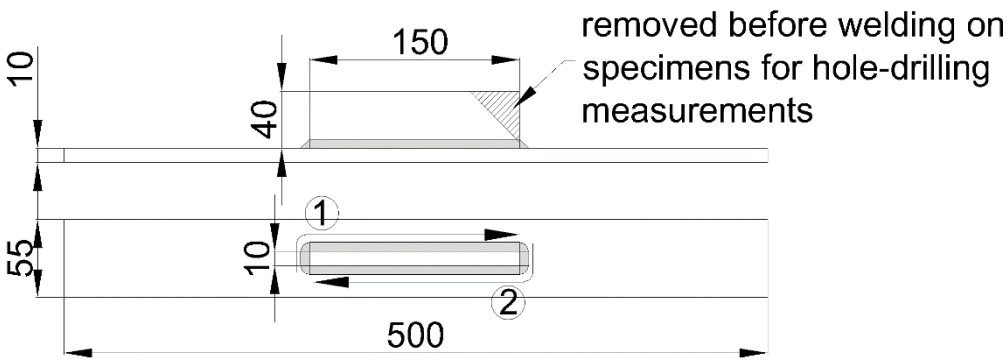


**Fig. 7** Longitudinal stiffener specimens, welding sequence indicated by ① and ②.

Residual stress measurements by the hole drilling method were done on three specimens. The measurements were done at the right end of the stiffener. The holes were distributed leaving at least 4 mm in between and so that they do not shadow each other with respect to the stiffener. Strain gauge rosettes of Type A according to ASTM E837 [14] were applied, respectively Type B when closer than 5 mm to the weld. The drill diameter was 1.6 mm. The drilling depth 1 mm. Depth increments were 0.01 mm up to a depth of 0.1 mm and then 0.05 mm. Fig. 8 shows exemplarily the residual stresses over the hole depth measured on a specimen at two different distances from the weld toe. The residual stress curves over depth were calculated by the integral method [15]. Furthermore, values according to ASTM E837-13 assuming a uniform residual stress distribution up to 1 mm depth are plotted. Transversal residual stresses show a steep increment on the first 0.1 mm and then stabilize on a value slightly higher than the result assuming a uniform distribution. The residual stress assessment close to the surface is sensitive to inaccuracies. Residual stresses may be underestimated due to uncertainties in the determination of the "zero" position where the cutter touches the specimen surface [14, 16] or a smaller hole diameter than measured at the end of drilling. The evaluation of the uniform residual stress distribution is less prone to errors and typically more accurate [16].

Further measurements were done by X-ray diffraction on three specimens. The measurements were executed by the Institute of Joining and Welding (ifs), TU Braunschweig. The X-ray measurements were performed on the centreline of the specimen.

The residual stresses measured by hole drilling and X-ray diffraction are compared to the simulation results in Fig. 9. Specimens 16 and 19 used for the X-ray measurements had a straight stiffener, specimen 5 had a bevelled stiffener (compare Fig. 7) as the specimens for hole drilling. When comparing the results of both measuring methods it has to be considered, that the measuring depth of the X-ray diffraction is approximately 5 µm, while the hole drilling measurements were evaluated over a depth of 1 mm. The results in Fig. 8 indicate that the transversal residual stresses increase on the first 0.1 mm from the surface. The specimens presented a rolling skin. For the hole drilling measurements the surface had to be slightly grinded with sandpaper in order to assure a proper installation of the strain gauge rosettes. Still, the results obtained with both methods are in good agreement beyond 5 mm from the weld. Closer to the weld, were welding residual stresses are expected to dominate over those resulting from the production or surface treatment of the plate,

transversal residual stresses show different trends. While the hole drilling results increase to over 300 MPa, the X-ray values show a maximum of about 200 MPa and decrease towards the weld. In the heat affected zone close to the weld material properties may differ from those of the base material. The accuracy of hole drilling measurements close to the weld may be affected by the vicinity to a step feature (the weld), the use of Type B strain gauge rosettes and residual stresses of more than 70% of yield strength [16]. On X-ray measurements close to the weld the measuring spot of 1-2 mm will in part cover weld material. Furthermore, measurements in transversal direction are limited to Ψ-angles of the same sign. These not ideal measuring conditions may have affected the results obtained with both methods. To what extent, cannot be definitely said without further investigations.

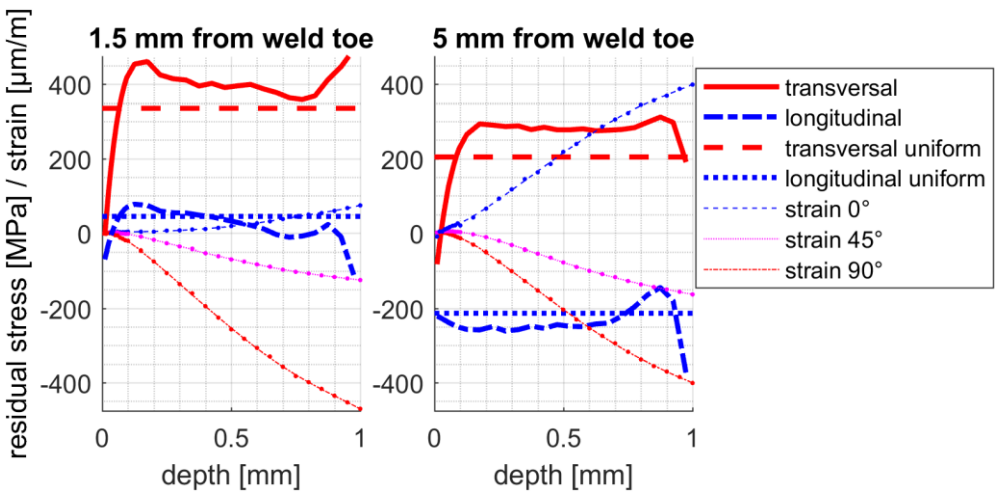


**Fig. 8** Residual stresses measured by hole drilling (specimen 1). Strains refer to their orientation relative to the weld (0° ≙ longitudinal).

In the simulation the mechanical boundary conditions were simplified by restraining the displacement in vertical direction at the ends of the model and relieving these restraints in the last load step, at room temperature. As mentioned in section 2.2.2, the calculated residual stresses should not be evaluated on the first 1 mm from the weld toe because of the singularity in the FE model. In both directions simulation results lay close to the hole drilling measurements. Both curves show an offset of about 2 mm compared to the measurements. This may indicate that too much energy was put into the model (compare Fig. 3 and Fig. 4).

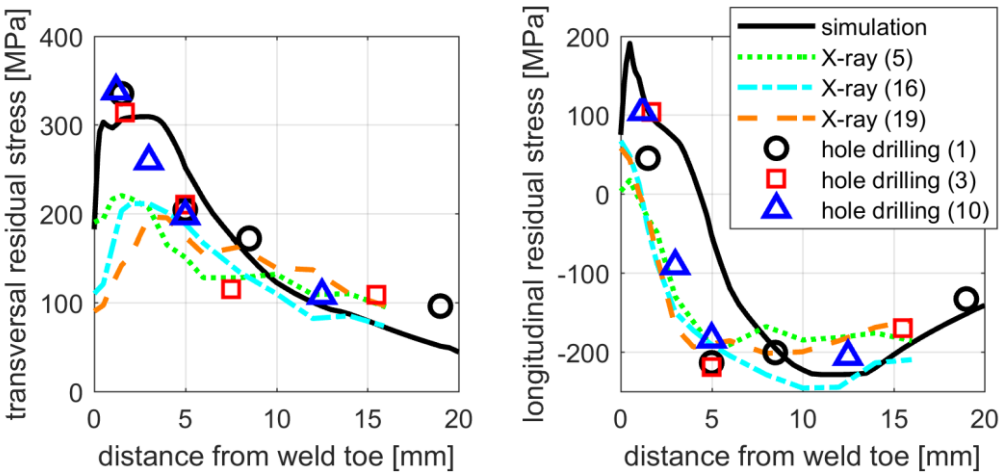


**Fig. 9** Calculated and measured residual stresses (numbers in brackets indicate the specimen number).

## K-BUTT WELD

Small-scale specimens with a K-butt weld between two plates of different thicknesses have been investigated in [7]. The dimensions of the geometry are shown in Fig. 10. A 10 mm plate was welded to a 25 mm plate using six weld passes as shown in the detail. Five specimens have been cut out of each plate using a band saw. Steel of grade S355J2C+N was used. Tensile tests of the 10 mm plate gave the following values: yield strength $R_{eH}$ = 394 MPa; tensile strength $R_m$ = 524 MPa; Young's modulus $E$ = 204 GPa.

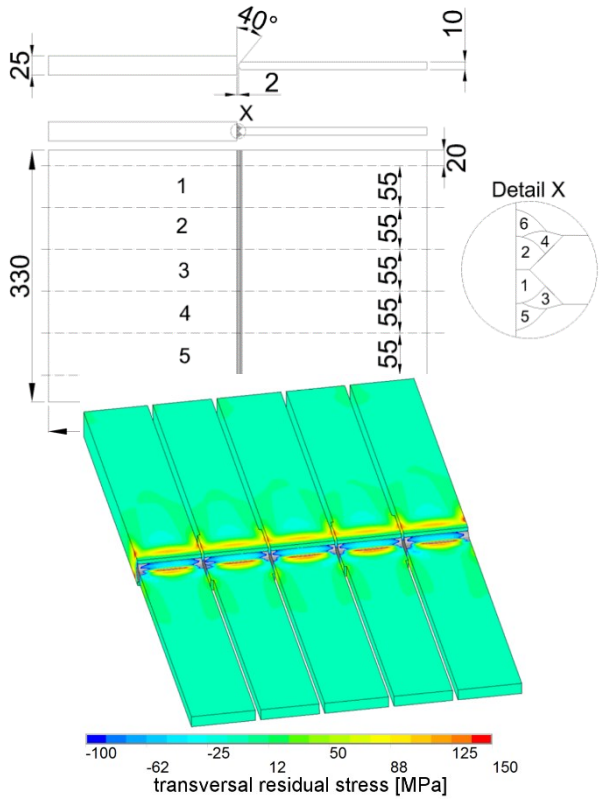


**Fig. 10** K-butt specimens (left) and calculated residual stresses (right) [7].

Welding simulations were performed with the approach described above. To simulate the cutting of the specimens the elements between the specimens were deactivated after cooling to room temperature. The resulting transversal residual stress distribution after cutting is plotted in Fig. 10 (right).

In Fig. 11 the calculated residual stresses on the upper side of the specimens are compared to measurements by X-ray diffraction and hole drilling. Measurements were performed on several specimens indicated in the legend of Fig. 11 by the number of the plate and of the specimen (1 to 5 according to Fig. 10). As mentioned in section 3.1 the X-ray diffraction and hole drilling methods have different measuring depths. Compared to the longitudinal stiffeners the X-ray measurements show a larger scatter. Measurements on specimen 23-5 are in agreement with the hole drilling results, the other two curves indicate lower values. The five curves for the simulation show the results on the five specimens cut out of one plate. Transversal residual stresses lay within the scatter of the hole drilling measurements up to 5 mm from the weld toe and slightly above it beyond this distance. Two of the X-ray measurements lay about 100 MPa below the simulation results. The third (specimen 23-5) shows values in the range of the hole drilling measurements and simulations up to 7 mm from the weld.

In longitudinal direction the simulation results follow the trend of the hole drilling measurements and the highest of the X-ray measurements (specimen 23-5) overestimating them by about 100 MPa.

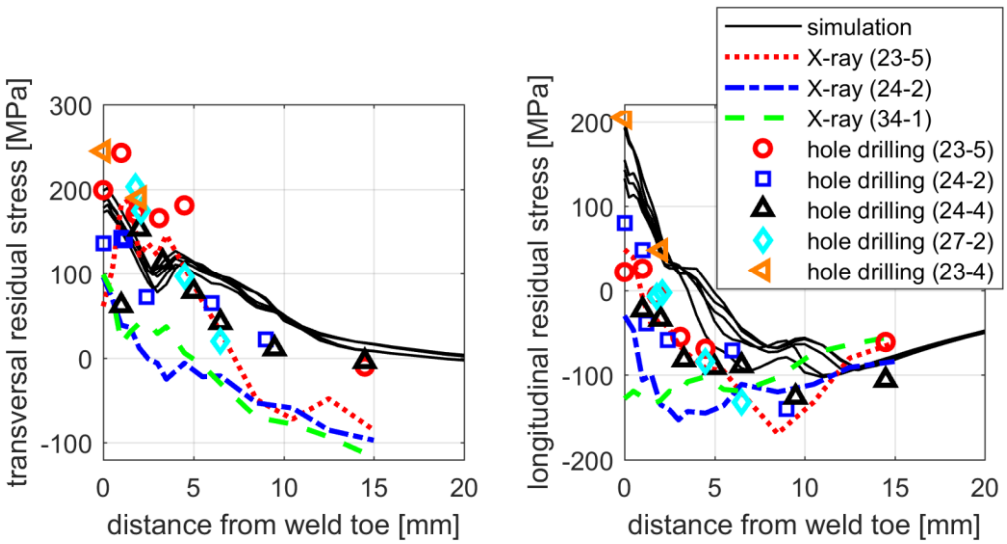


**Fig. 11** Calculated and measured residual stresses on the upper side of the k-butt weld specimens (numbers in brackets indicate the specimen number) [7].

## LARGE-SCALE COMPONENT

In [17] residual stresses on structure-like components have been investigated. The investigated geometry is shown in Fig. 12. It included a cruciform joint and a longitudinal stiffener as shown in the detail (Fig. 12, right). The plate thickness was 20 mm for the girder and 16 mm for the stiffener. In the welding sequence the right stiffener and the right side of the cruciform joint (detail in Fig. 12) were welded last. The applied steel was of shipbuilding grade A36 with a yield strength of $R_{eH}$ = 430 MPa and tensile strength $R_m$ = 555 MPa (determined in tensile tests of the 20 mm material).

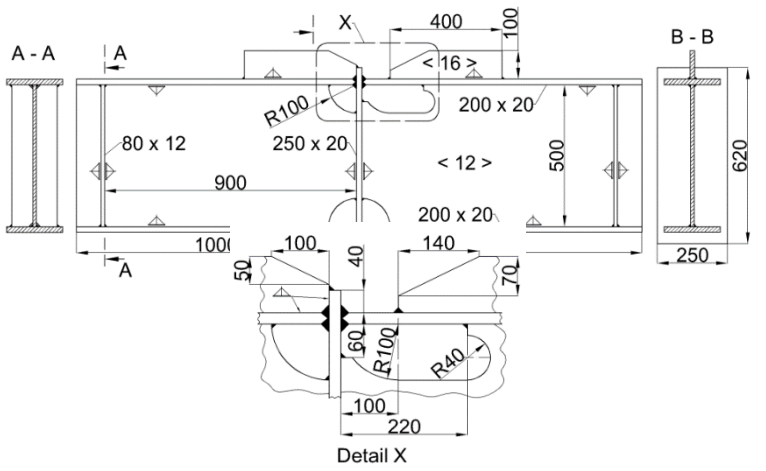


**Fig. 12** Dimensions of the large-scale component [17].

Residual stresses were measured by X-ray diffraction at ifs, TU Braunschweig. Fig. 13 shows the results from two specimens along with the corresponding calculated residual stresses. The measurements were performed at the centreline of the specimens between the cruciform joint and the longitudinal stiffener. The indicated distance refers to the weld toe of the cruciform joint. The weld toe of the longitudinal stiffener is located at the right side of the diagrams (at 75 mm). Simulation and measurement results for two specimens are shown. On specimen M3 the cruciform joint was welded with a total of 10 weld passes, on specimen M4 with 15. On the latter specimen the last weld beads were applied on top of the weld, a few millimetres from the weld toe at the horizontal girder (comparable to weld pass 6 in the detail of Fig. 10). In this manner two different residual stress distributions were achieved. Whereas on specimen M3 transversal residual stresses decrease to zero at the cruciform joint (left side of the diagram), on specimen M4 they rise to about 200 MPa.

The simulations were performed with the procedure describe above. Stress-strain curves with a yield strength of 430 MPa at room temperature, as on the actual specimens, were used. For higher temperatures the curves have been scaled as described in section 2.2.5. Welding speeds were determined based on thermocouple measurements prior to perform the simulations, these values were used for the simulations: 7.1 mm/s on the side of the longitudinal stiffener and 10 mm/s at its end; between 5.3 and 8.3 mm/s for the cruciform joint in specimen M3 and 7.8 mm/s in specimen M4. As shown in [7] the applied welding speed does not significantly influence the resulting residual stresses. In [18] it was observed for the cruciform joint that the residual stresses calculated on the plate surface depend mostly on the last applied weld beads. It is therefore assumed that a fixed welding speed (7.8 mm/s) would have resulted in the same residual stress distributions.

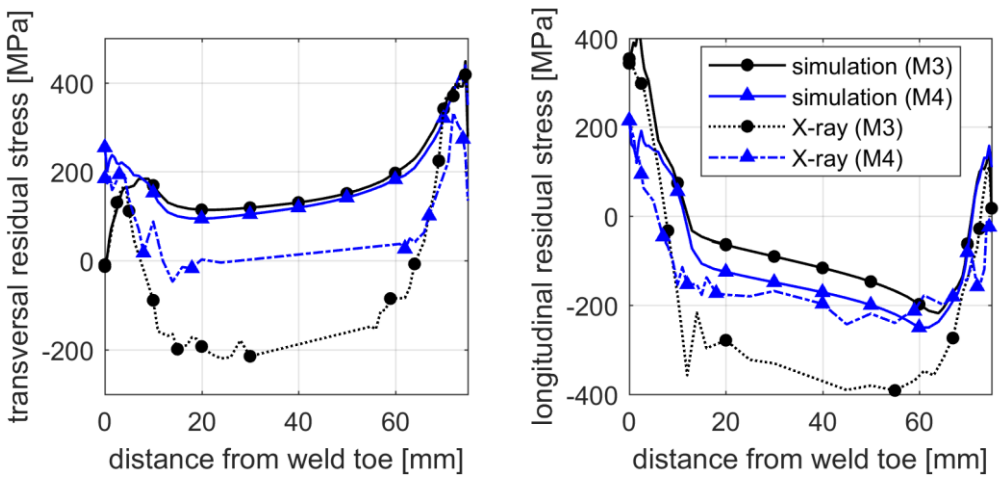


**Fig. 13** Calculated and measured residual stresses between cruciform Joint (distance = 0 mm) and longitudinal stiffener (distance = 75 mm) (M3 and M4 indicate specimen number according to [17]).

The comparison of the simulation results to the measurements (Fig. 13) shows a relatively good agreement at the ends of the measuring path (up to 5 mm from both welds) and a large difference in the middle (5 to 70 mm). This was due to compressive residual stresses up to -300 MPa on the plate surface resulting from blast cleaning. Specimen M4 had been stress relieved before welding and these compressive residual stresses were reduced to -50 MPa. In the zones heated by the welds the residual stresses present in the plate were relieved and the welding residual stresses prevailed.

## CONCLUSIONS

A welding simulation approach for metal active gas welding using a uniform temperature heat source without calibration and a simplified consideration of phase transformation was applied to a longitudinal stiffener. Simulation parameters were varied to show their influence on the calculated residual stresses. Simulation results and residual stress measurements on three different welded geometries were compared for validation.

The following is concluded from the results:

- With the applied simulation approach a variation in heat input does not significantly affect the amount of residual stresses calculated on the plate surface at a longitudinal stiffener. No influence of the temperature interval for phase transformation during cooling was observed. The variation of yield strength did affect the resulting residual stresses. If the objective are the residual stresses in front of the weld, for this particular weld geometry, the heat input appears to be of less importance than mechanical material properties.
- Residual stress measurements by X-ray diffraction and holed drilling showed large differences. Especially on the longitudinal stiffener transversal residual stresses measured by X-ray diffraction were lower than the hole drilling results.

- The calculated residual stresses lay within the scatter of the hole drilling measurements. On the small-scale specimens the values were about 100 MPa higher than the X-ray diffraction measurements. Different residual stress distributions due to the changed weld pass arrangement at the cruciform joint of the large-scale component could be determined by the simulations.
- Based on the results, the presented simulation approach appears suitable to predict residual stresses from MAG welding in low alloy steels at least qualitatively ($\pm$100 MPa). This applies only to residual stresses on the plate surface in front of the weld. Residual stress distributions over the plate thickness or distortions have not been verified. Considering the uncertainties in the measurements, this result seems acceptable.

## ACKNOWLEDGEMENTS

The presented research was funded by the Deutsche Forschungsgemeinschaft (DFG, German Research Foundation) – EH 485/4-1.

## REFERENCES

[1] J.-D. CAPRACE, G. FU, J. F. CARRARA, H. REMES, S. B. SHIN: 'A benchmark study of uncertainness in welding simulation', *Marine Structures*, Vol. 56, pp. 69-84, 2017.

[2] L.-E. LINDGREN: *Computational welding mechanics - Thermomechanical and microstructural simulations*, Woodhead Publishing in Materials, Cambridge, 2007.

[3] C. HEINZE, C. SCHWENK, M. RETHMEIER: 'Effect of heat source configuration on the result quality of numerical calculation of welding-induced distortion', S*imulation Modelling Practice and Theory*, Vol. 20, pp. 112-123, 2012.

[4] A. BELITZKI, C. MARDER, A. HUISSEL, M. F. ZAEH: 'Automated heat source calibration for the numerical simulation of laser beam welded components', *Prod. Eng. Res. Devel.*, Vol. 10, pp. 129-136, 2016.

[5] J. KLASSEN: *Beitrag zur vereinfachten Eigenspannungsberechnung von Mehrlagenschweißverbindungen [Contribution to simplified residual stress calculations for multilayer welds, in German]*, dissertation, TU-Braunschweig, 2018.

[6] J. A. GOLDAK AND M. AKHLAGHI: *Computational welding mechanics*, Springer, New York, 2005.

[7] N. FRIEDRICH and S. EHLERS: 'A simplified welding simulation approach used to design a fatigue test specimen containing residual stresses', *Ship Technology Research*, to be published 2018.

[8] J. GOLDAK, A. CHAKRAVARTI, M. BIBBY: 'A new finite element model for welding heat sources', *Metallurgical Transactions B*, Vol. 15, pp. 299-305, 1984.

[9] J. B. ROELENS, F. MALTRUD, J. LU: 'Determination of residual stresses in submerged arc multi-pass welds by means of numerical simulation and comparison with experimental measurements', *Welding in the World*, Vol. 33, No. 3, pp. 152-159, 1994.

[10] L.-E. LINDGREN, H. RUNNEMALM, M. O. NÄSSTRÖM: 'Simulation of multipass welding of a thick plate', *Int. J. for Numerical Methods in Engineering*, Vol. 44, No. 9, pp. 1301-1316, 1999.

[11] VEREIN DEUTSCHER INGENIEURE, EDITOR: *VDI heat atlas. 2nd ed.*, Springer, Berlin, 2010.

[12] M. WICHERS: S*chweißen unter einachsiger, zyklischer Beanspruchung – Experimentelle und numerische Untersuchungen [Welding under uniaxial cyclic loads – Experimental and numerical research, in German]*, dissertation, TU-Braunschweig, 2006.
[13] K. DILGER AND T. WELTERS, EDITORS: *Schlussbericht zum BMBF-Verbundprojekt SST – Schweißsimulationstool [Report to the BMBF-project SST – welding simulation tool, in German]*, Shaker Verlag, Aachen, 2006.
[14] ASTM *E837-13a. Standard test method for determining residual stresses by the hole-drilling strain-gage method*, ASTM International, West Conshohocken (PA), 2013.
[15] G. SCHAJER: 'Measurement of non-uniform residual stresses using the hole drilling method', *J. of Engineering Materials and Technology*, Vol. 110, No. 4, Part I pp. 338-343, Part II pp. 344-349, 1988.
[16] G. S. SCHAJER, EDITOR: *Practical residual stress measurement methods*, Wiley, Chichester (UK), 2013.
[17] J. KLASSEN, N. FRIEDRICH, W. FRICKE, T. NITSCHKE-PAGEL, K. DILGER: 'Influence of residual stresses on fatigue strength of large scale welded assembly joints', *Welding in the World*, Vol. 61, pp. 361-374, 2017.
[18] J. KLASSEN, N. FRIEDRICH, W. FRICKE, T. NITSCHKE-PAGEL, K. DILGER: *Entwicklung von Methodiken zur Bewertung von Eigenspannungen an Montagestößen bei Stahl-Großstrukturen. AiF-Schlussbericht. IGF-Vorhaben 17652N [Development of methods for evaluation of residual stresses in assembly joints of large steel structures. AiF-report. IGF-project 17652N, in German]*, 2016.